Optimal Placement of STATCOMs for Improving Voltage Stability in Industrial Power Systems

Hyeonseong Mun
Korea Electric Power Corporation (KEPCO)
Naju, South Korea

***Abstract*—This paper presents a methodology for enhancing voltage stability in industrial power systems by optimizing the placement of Static Synchronous Compensators (STATCOMs). A fixed-point iterative solver is developed in MATLAB for analyzing unbalanced multi-voltage networks under steady-state conditions. To determine optimal STATCOM placement, metaheuristic algorithms—Particle Swarm Optimization, Genetic Algorithm, and Pattern Search—are sequentially applied to minimize reactive power demand subject to voltage constraints at critical load buses. The proposed solutions are validated in OpenDSS, confirming consistency in bus voltages and power flows across frameworks. Simulation results show that multiple STATCOM installations near load buses significantly enhance voltage stability and reduce the compensation requirement by 67.81% compared to a single installation. The combined use of analytical modeling, optimization, and simulation provides a robust framework for deploying STATCOMs in industrial systems.**

***Index Terms*—Static synchronous compensator (STATCOM), industrial power systems, voltage stability improvement, optimal placement, metaheuristic optimization algorithm.**

I. Introduction

The ongoing electrification of industrial systems has significantly increased the deployment of advanced and power-electronics-based loads. These devices are inherently sensitive to power quality disturbances which can result in equipment malfunctions, operational downtime, and significant financial losses [1]. As industries pursue improved energy efficiency and carbon reduction targets, voltage stability has become an increasingly critical aspect of reliable system operation [2].

Among various mitigation technologies, static synchronous compensators (STATCOMs) have gained prominence as effective solutions for dynamic reactive power support and voltage regulation. Their fast response time and modular architecture make them well-suited for industrial distribution networks, where load unbalance and multiple voltage levels exist [3].

However, due to installation costs, space constraints, and regulatory limitations, deploying STATCOMs indiscriminately is impractical. Instead, optimal placement strategies are essential to maximize system performance with limited resources. Most existing approaches address the STATCOM placement problem using a single optimization technique and provide limited validation of the obtained results, particularly in terms of solution robustness and modeling consistency [3]–[5].

To address these limitations, this paper proposes a sequential metaheuristic framework for optimal STATCOM placement and sizing under steady-state operating conditions. The approach is implemented in MATLAB and cross-validated with OpenDSS, forming a hybrid simulation environment to ensure modeling accuracy and solution consistency. By strategically combining algorithms effective in global exploration and local refinement, the method improves overall optimization performance.

II. Modeling of STATCOM and Industrial Feeder

This section covers the design of a STATCOM and an industrial grid to determine optimal installation locations.

A. Topology of STATCOM

A STATCOM consists of five main components: voltage source inverters (VSIs), AC harmonic filters, coupling transformers, a DC-link, and a control block [6]. An overview of this structure is presented in Fig. 1.

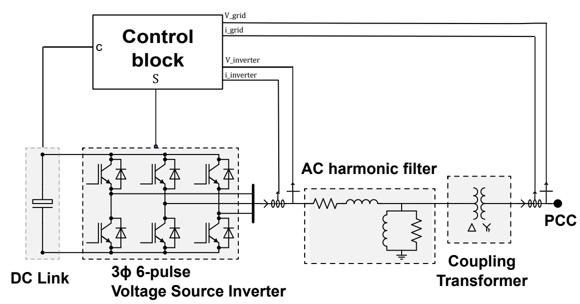

Fig. 1. Functional configuration of the STATCOM system

- **Voltage Source Inverter**: Converts DC voltage into AC and enables reactive power exchange. It regulates voltage magnitude and phase to control reactive power.
- **AC Harmonic Filter**: Suppresses high-frequency harmonics and improves power quality. It consists of a series reactor with a damping resistor and a parallel RLC branch.
- **Coupling Transformer**: Matches voltage levels between the VSI and the grid, enables reactive power injection at the PCC, and provides electrical isolation.
- **DC-Link**: Maintains stable DC voltage for inverter operation using capacitors or independent energy storage. It defines the inverter's voltage capability and may be supported by auxiliary sources under abnormal conditions.
- **Control Block**: The control system applies a feedback-based voltage regulation scheme through controlled reactive current injection. The voltages at the point of common coupling are measured and transformed using the Park–Clarke transformation and a phase-locked loop. The resulting voltage deviation from the reference is fed back to regulate reactive power injection through pulse-width modulation.

979-8-3315-8138-1

B. Modeling of Industrial Test System

An industrial test system is developed to evaluate voltage regulation under various STATCOM placements. It comprises two power supplies, transmission and distribution lines, and induction motors installed at industrial load buses.

1) Benchmarking System: The benchmarking system consists of multiple voltage levels and unbalanced loading conditions. Its topology and component specifications are illustrated in Fig. 2 and summarized in Table I [7].

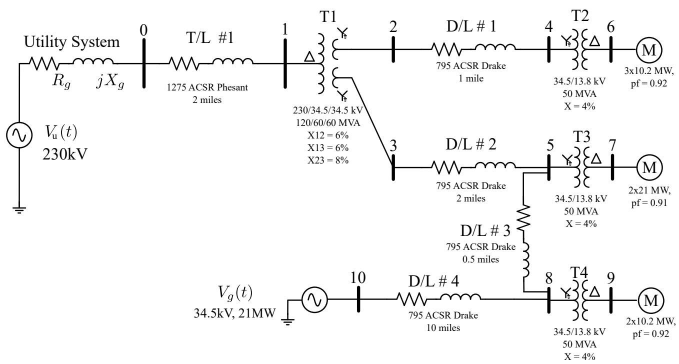

Fig. 2. Industrial test system topology

TABLE I
INDUSTRIAL SYSTEM SPECIFICATIONS

Component	Specifications
Power Source	
Generator 1 (V_{u})	
Voltage	230 [kV] (3-phase, 60 [Hz])
Short-Circuit Capacity	$3\phi/1\phi$ = 4500/3000 [MVA]
X/R Ratio	X_1/R_1 = X_0/R_0 = 15
Generator 2 (V_{g})	
Voltage / Active Power	34.5 [kV] (3-phase, 60 [Hz]) / 21 [MW]
Transformer Specifications	
Transformer 1 for Buses (1-3)	
Connection	Δ - Y - Y
Voltage Rating	230 / 34.5 / 34.5 [kV]
Power Rating	120 / 60 / 60 [MVA]
Percent Impedance (%Z)	$X_{12} = 6\%$, $X_{13} = 6\%$, $X_{23} = 8\%$
Transformers 2, 3, and 4 for Buses (4, 6), (5, 7), and (8, 9)	
Connection	Y - Δ
Voltage Rating	34.5 / 13.8 [kV]
Power Rating / %Z	50 [MVA] / $X_t = 4\%$
Transmission Line	
# 1 (2 miles)	1275 kcmil ACSR Phesant (Phases)
Distribution Line	
# 1 (1 mile), # 2 (2 miles),	795 kcmil ACSR Drake (Phases)
# 3 (0.5 mile), # 4 (10 miles)	266.8 kcmil ACSR Waxwing (Neutral)
Industrial Load	
Motor 1–3 at Bus 6	10.2 [MW] with PF 0.92, 3 motors
Motor 4, 5 at Bus 7	21.0 [MW] with PF 0.91, 2 motors
Motor 6, 7 at Bus 9	10.2 [MW] with PF 0.92, 2 motors

2) System Modeling: The system is modeled using the nodal admittance method, which defines the steady-state relationship between complex bus voltages and currents as:

$$\mathbf{I} = \mathbf{Y}_{\mathrm{system}}\mathbf{V} \tag{1}$$

In this formulation, $\mathbf{I} \in \mathbb{C}^n$ and $\mathbf{V} \in \mathbb{C}^n$ denote the complex current injection and voltage vectors at n network nodes, respectively. The global admittance matrix $\mathbf{Y}_{\mathrm{system}} \in \mathbb{C}^{n\times n}$ captures the electrical topology of the system and is assembled from the admittance contributions of the following components:

- **Transmission and Distribution Lines:** Designed using multi-phase impedance models based on conventional geometry [8], [9]. Each segment is assembled into the global admittance matrix using incidence mapping.
- **Transformers:** Modeled using primitive admittance matrices derived from short-circuit impedance, capturing leakage reactance and phase shift characteristics associated with wye-delta and other winding configurations [10].

The line admittance matrix Y_{line} and transformer admittance matrix Y_{xfmr} are incorporated into the global admittance matrix Y_{system} by aggregating the contributions of all line and transformer elements at their corresponding node locations [11]. This mapping-based assembly is expressed as:

$$Y_{\mathrm{system}}(i,j) = \sum_{(a,b)\in\mathcal{L}} Y_{\mathrm{line}}^{(a,b)}(i,j) + \sum_{(m,n)\in\mathcal{T}} Y_{\mathrm{xfmr}}^{(m,n)}(i,j) \tag{2}$$

where:

- $Y_{\mathrm{line}}^{(a,b)}(i,j)$: Contribution to (i,j) from the line between node a and b
- $Y_{\mathrm{xfmr}}^{(m,n)}(i,j)$: Contribution to (i,j) from the transformer between node m and n
- $\mathcal{L}$: Set of all line segments indexed by node pairs (a,b)
- $\mathcal{T}$: Set of all transformer connections indexed by node pairs (m,n)

After assembling all component admittances, the nodal admittance matrix Y_{system} provides the foundation for steady-state power flow analysis and optimization under unbalanced, multi-phase operating conditions. Loads and STATCOMs are represented as constant-PQ elements, while two generators are modeled as slack and PV nodes, regulating voltage magnitude and supplying fixed real power, respectively.

III. Optimal Placement Strategies for STATCOMs

This section presents a unified framework for optimal STATCOM placement in industrial systems, integrating a fixed-point method with metaheuristic optimization algorithms. The framework ensures computational efficiency and reliable performance under practical voltage constraints, supporting both centralized and distributed placement strategies. Validation is performed through cross-platform comparison with OpenDSS.

A. Power Flow Solution

A fixed-point method solves unbalanced multi-phase power flow. Buses are classified as slack, PV, or PQ, enabling efficient analysis under practical conditions.

1) Fixed-Point Power Flow Method: The fixed-point method solves power flow equations in unbalanced systems by iteratively updating bus voltages based on the mismatch between specified power injections and computed nodal currents [12]. Assuming a constant PQ model for all loads and STATCOMs, the injected current at each iteration k is computed as:

$$I_{\mathrm{inj}}^{(k)} = -\left(\frac{S}{V^{(k)}}\right)^{*} \tag{3}$$

979-8-3315-8138-1

The system admittance matrix is partitioned to isolate unknown voltages, which are updated using a transformation matrix derived from network topology. The process repeats until voltage convergence is achieved, as detailed in Algorithm 1.

Algorithm 1 Fixed-Point Power Flow Solution

Require: System admittance matrix Y_{system}; complex power injections S; convergence threshold ϵ

Ensure: Converged nodal voltage vector $\mathbf{V}^{(k)}$

Initialize: Set flat-start voltage profile $V_i^{(0)} = 1\angle\theta_i$, where $\theta_i \in \{0°, -120°, 120°\}$ corresponds to phase a, b, and c

Assign: Fix voltages for slack buses and grounded neutrals

Partition: Decompose Y_{system} into submatrices $Y_{11}, Y_{12}, Y_{21}, Y_{22}$, based on known and unknown voltage/current nodes $(V_{\text{known}}, V_{\text{unknown}}, I_{\text{known}}, I_{\text{unknown}})$

Compute: Construct transformation matrix H_{bus} as:

$$H_{11} = Y_{11} - Y_{12}Y_{22}^{-1}Y_{21}, \quad H_{12} = Y_{12}Y_{22}^{-1},$$
$$H_{21} = -Y_{22}^{-1}Y_{21}, \quad H_{22} = Y_{22}^{-1}$$

Set iteration counter $k \leftarrow 0$

repeat

Compute injected current: $I_{\text{inj}}^{(k)} = -\left(\frac{S}{V^{(k)}}\right)^*$

Form known/unknown voltage and current vectors

Update unknowns:

$$\begin{bmatrix} V_{\text{unknown}} \\ I_{\text{unknown}} \end{bmatrix} = \begin{bmatrix} H_{11} & H_{12} \\ H_{21} & H_{22} \end{bmatrix} \begin{bmatrix} V_{\text{known}} \\ I_{\text{known}} \end{bmatrix}$$

$k \leftarrow k + 1$

until $\left\| V^{(k)} - V^{(k-1)} \right\|_\infty < \epsilon$

Return: Converged nodal voltage vector $\mathbf{V}^{(k)}$

2) Bus Classification: Buses in the system are categorized as slack, PV, or PQ types based on the set of known and unknown electrical quantities, as summarized in Table II.

TABLE II
BUS TYPE CHARACTERISTICS

Bus Type	Known	Unknowns	Assigned Buses
Slack (Reference)	$\lvert V\rvert$, $\angle\theta$	P, Q	Bus 0
PV (Generator)	P, $\lvert V\rvert$	Q, $\angle\theta$	Bus 10
PQ (Load)	P, Q	$\lvert V\rvert$, $\angle\theta$	Buses 6, 7, and 9

Bus 0 is designated as the slack bus, providing a reference voltage magnitude and angle. Bus 10 operates as a PV bus, maintaining a specified voltage magnitude through active power injection. Buses 6, 7, and 9 are modeled as PQ buses with constant power demand. The STATCOM bus is also treated as a PQ bus with zero active power, while the reactive power is adjusted dynamically according to simulation conditions.

B. Evaluation Methodologies

STATCOM placements in industrial systems are constrained by capital costs, site limitations, and regulatory requirements. Hazardous zones are excluded, necessitating a fixed number of STATCOMs at predefined candidate buses [13].

1) Single Installation: A STATCOM is installed at a candidate bus to provide centralized voltage support. While this setup simplifies control and lowers cost, effectiveness diminishes with distance from critical loads. Simulations increase reactive output in 1 Mvar steps until voltages at load buses reach 1.00 p.u., yielding required reactive power and voltage profiles.

2) Multiple Installations: Multiple STATCOMs are deployed across selected buses (e.g., Bus 1–9) to enhance localized voltage regulation. To identify optimal placements and reactive power ratings, three optimization techniques are employed: Particle Swarm Optimization (PSO), Genetic Algorithm (GA), and Pattern Search (PS), which offer global exploration and local refinement capabilities.

C. Optimization Algorithm

A constrained optimization problem is formulated to minimize total reactive power injected by STATCOMs, while maintaining voltage levels above threshold values at load buses.

- **Objective Function:**

$$\min_{\mathbf{x}} f(\mathbf{x}) = \sum_{i=1}^{N} Q_i, \quad \mathbf{x} = [Q_1, Q_2, \ldots, Q_N] \tag{4}$$

where Q_i is the injected reactive power by STATCOM at bus i.

- **Voltage Constraints:**

$$V_k \geq 1.00 \text{ p.u.}, \quad \forall k \in \{6, 7, 9\} \tag{5}$$

To address the non-convex and constrained nature of the optimization problem, three metaheuristic algorithms are employed: PSO, GA, and PS. Each adopts a distinct strategy for global or local search and can be applied either individually to exploit distinct search behaviors or sequentially for refinement.

1) Particle Swarm Optimization: Each particle represents a candidate solution $\mathbf{x}_i = [Q_1, Q_2, \ldots, Q_N]$. The position and velocity of each particle are updated as follows [14]:

$$\mathbf{v}_i^{(t+1)} = \omega\mathbf{v}_i^{(t)} + c_1u_1(\mathbf{p}_i - \mathbf{x}_i^{(t)}) + c_2u_2(\mathbf{g} - \mathbf{x}_i^{(t)}) \tag{6}$$
$$\mathbf{x}_i^{(t+1)} = \mathbf{x}_i^{(t)} + \mathbf{v}_i^{(t+1)} \tag{7}$$

where $\mathbf{v}_i^{(t)}$ denotes the velocity of particle i at iteration t, $\mathbf{p}_i$ denotes the best position visited by particle i, and $\mathbf{g}$ denotes the global best position among all particles. The random variables u_1 and u_2 are independently and uniformly distributed in $[0, 1]$. A penalty function is incorporated to enforce voltage limits.

2) Genetic Algorithm: GA evolves a population of candidate solutions $\mathbf{x}_i = [Q_1, Q_2, \ldots, Q_N]$ through selection, crossover, and mutation. The crossover operation is defined as [15]:

$$\mathbf{x}_{\text{child}} = \alpha\mathbf{x}_i + (1 - \alpha)\mathbf{x}_j, \quad \alpha \sim \mathcal{U}(0, 1) \tag{8}$$

Mutation is applied to each gene as:

$$x'_j = x_j + \delta_j, \quad \delta_j \sim \mathcal{U}(-\varepsilon, \varepsilon) \tag{9}$$

Parent selection is typically performed using tournament or roulette-wheel selection based on fitness values. Mutation introduces random variation in the offspring to maintain genetic diversity and prevent premature convergence.

Violations are managed using a penalized fitness function:

$$f_{\text{penalized}}(\mathbf{x}) = f(\mathbf{x}) + \lambda \sum_k \max(0, 1.00 - V_k) \tag{10}$$

The algorithm iterates through generations until convergence or a predefined iteration limit is met.

979-8-3315-8138-1

3) Pattern Search: PS is a derivative-free optimization algorithm that iteratively explores neighboring points around a current solution $\mathbf{x}_k$ using a set of polling directions $\mathcal{D}$ [16]:

$$\mathbf{x}_{\text{trial}} = \mathbf{x}_k + \Delta_k d, \quad d \in \mathcal{D} \tag{11}$$

The size of the mesh Δ_k is adaptively adjusted according to objective improvement, allowing an efficient search without gradients. This makes PS suitable for non-smooth or black-box problems. Voltage constraints are imposed using an augmented Lagrangian approach by adding penalty terms for voltage limit violations to the objective function, thereby guiding the search toward feasible solutions by penalizing constraint violations without altering the underlying search structure.

Table III presents a comparative summary of the three algorithms highlighting their core features, constraint-handling approaches, and computational characteristics. PSO exhibits rapid convergence, GA maintains solution diversity, and PS offers robust local refinement without derivative dependence.

TABLE III
COMPARISON OF OPTIMIZATION ALGORITHMS FOR PLACEMENT

Feature	PSO	GA	PS
Search Type	Swarm-based	Evolutionary	Local polling
Exploration	Global + local	Global	Local only
Constraints	Penalty function	Penalized fitness	Augmented Lagrangian
Key Parameters	ω, c_1, c_2	Mutation, crossover rate	Mesh size Δ_k
Convergence	Velocity stagnation	Generation limit	Mesh size tolerance
Pros	Fast, balanced	Diverse solutions	Simple, robust
Cons	Risk of local minima	Slower, parameter tuning	Risk of local optima

D. Simulation and Validation Framework

A two-stage simulation framework was developed to identify and validate optimal STATCOM placements. In the first stage, unbalanced multi-phase power flow analysis was conducted in MATLAB using a fixed-point solver integrated with meta-heuristic optimization algorithms such as PSO, GA, and PS for determining placement and reactive sizing.

In the second stage, model consistency was validated through comparison of results obtained from MATLAB and OpenDSS under identical network topology and loading conditions. Agreement between the two solutions was confirmed across key performance metrics:

- Nodal admittance matrix Y_{system}
- Bus voltage magnitudes and phase angles
- Branch currents in transmission and distribution lines
- Active and reactive power exchange by sources and loads

This coordinated framework combines MATLAB's optimization flexibility with OpenDSS's detailed modeling capabilities, ensuring both computational efficiency and physical accuracy for industrial power system analysis.

IV. SIMULATION RESULTS AND VALIDATION

This section presents simulation results evaluating STATCOM performance under various installation strategies. Both single and multiple placements are examined to assess voltage regulation across the network. Results are validated using OpenDSS to ensure consistency with MATLAB calculations.

A. Case Study 1: Single Installation

A single STATCOM was installed at each candidate bus (Bus 1–9), excluding the slack and PV buses. The STATCOM reactive power output was increased until all load-bus voltages (Buses 6, 7, and 9) were above 1.00 p.u.. Fig. 3 presents the resulting voltages and required reactive power, where subscripts a, b, and c denote phases (e.g., 6a indicates Phase a of Bus 6).

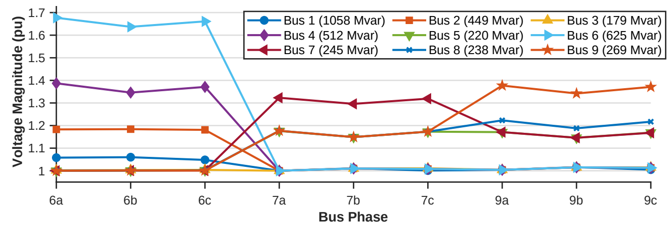

Fig. 3. Load Bus Voltages with Single STATCOM Installation

Simulation results demonstrate that both voltage magnitudes and reactive power demands are highly sensitive to STATCOM placement. Installing a STATCOM at Bus 6 yields the most severe overvoltage, with Bus 6a reaching 1.677 p.u. despite injecting 625 Mvar. Similarly, placement at Bus 4 causes Bus 6a to rise to 1.387 p.u. with 512 Mvar. These results reflect significant voltage amplification near the installation point, which can lead to violation of voltage limits.

In contrast, placing the STATCOM at an electrically remote location such as Bus 1—near the service entrance and distant from major loads—yields more uniform voltage improvement across the network. However, this configuration requires substantially higher reactive power (up to 1058 Mvar) due to the increased electrical distance from load centers.

Based on these observations, two key challenges are identified in single STATCOM installation:

- **Overvoltage risk** at or near the STATCOM bus, especially in cases of local reinforcement (e.g., Bus 4 or 6).
- **Inefficient voltage support** from remote placements (e.g., Bus 1), which require excessive capacity for improvement.

Among all candidates, Bus 3 provides the most effective balance between voltage regulation and reactive power efficiency. It achieves flat voltage profiles across Bus 6, 7, and 9 with only 179 Mvar, demonstrating that placing the STATCOM between the main reactive loads and the service entrance offers optimal performance without overvoltage or excessive compensation.

B. Case Study 2: Multiple Installations

For multi-STATCOM installations, PSO, GA, and PS algorithms were used to optimize placement and sizing. PS was applied sequentially using PSO and GA solutions as initial guesses. All optimal configurations placed STATCOMs near load buses (Bus 6, 7, and 9), highlighting the benefit of proximity for voltage regulation. Among standalone methods, PSO performed best, while the sequential combinations PSO-PS and GA-PS demonstrated superior overall performance. Table IV summarizes the comparative results, where Δ denotes the percentage reduction in total reactive power from the optimal single-installation case at Bus 3 with 179 Mvar.

979-8-3315-8138-1

TABLE IV
OPTIMIZED STATCOM PLACEMENT RESULTS

Algorithm	Bus	Phase a	Phase b	Phase c	Q (BUS)	Δ (%)
PSO	Bus 6	1.0007	1.0000	1.0034	**57.66 [Mvar]**	**67.79**
	Bus 7	1.0000	1.0009	1.0096	16.44(6), 25.93(7),	
	Bus 9	1.0004	1.0017	1.0103	15.29(9)	
GA	Bus 6	1.0010	1.0003	1.0037	**58.50 [Mvar]**	**67.32**
	Bus 7	1.0010	1.0018	1.0105	16.50(6), 26.00(7),	
	Bus 9	1.0021	1.0032	1.0119	16.00(9)	
PSO-PS GA-PS	Bus 6	1.0007	1.0000	1.0034	**57.62 [Mvar]**	**67.81**
	Bus 7	1.0000	1.0009	1.0096	16.43(6), 25.98(7),	
	Bus 9	1.0003	1.0016	1.0102	15.21(9)	
PS	Bus 6	1.0007	1.0000	1.0034	**58.89 [Mvar]**	**67.10**
	Bus 7	1.0046	1.0052	1.0141	16.27(6), 29.4(7),	
	Bus 9	1.0000	1.0012	1.0098	13.22(9)	

C. Case Study 3: Multiple Installations with Constraints

This case considers constraints under which STATCOM installation at major load buses is not permitted due to safety, environmental, or spatial limitations. Accordingly, Bus 6, 7, and 9, which represent the primary load buses, are excluded from the STATCOM installation candidate set. The placement and sizing outcomes are summarized in Table V.

TABLE V
OPTIMIZED STATCOM PLACEMENT RESULTS WITH CONSTRAINTS

Algorithm	Bus	Phase a	Phase b	Phase c	Q (BUS)	Δ (%)
PSO PSO-PS	Bus 6	1.0017	1.0000	1.0037	**82.88 [Mvar]**	**53.70**
	Bus 7	1.0019	1.0000	1.0099	26.15(4),	
	Bus 9	1.0056	1.0051	1.0143	56.73(5)	
GA GA-PS	Bus 6	1.0017	1.0000	1.0037	**82.85 [Mvar]**	**53.72**
	Bus 7	1.0019	1.0000	1.0099	26.15(4),	
	Bus 9	1.0056	1.0051	1.0143	56.70(5)	
PS	Bus 6	1.0018	1.0000	1.0037	**85.41 [Mvar]**	**52.28**
	Bus 7	1.0020	1.0000	1.0099	26.15(4),	
	Bus 9	1.0187	1.0155	1.0264	9.26(5), 50.00(8)	

In the constrained simulation scenario, the GA algorithm exhibited the best performance. The minor discrepancies observed in comparison with PSO are likely due to differences in how each algorithm handles decimal precision. These results suggest that GA effectively identified a near-optimal solution, thereby limiting the potential for further improvement during the subsequent PS-based refinement process.

D. Validation with OpenDSS

To validate the MATLAB-based results, four representative cases were selected from the previously defined base case and Case Studies 1–3. These cases were re-simulated in OpenDSS to obtain voltage magnitudes. The resulting voltage errors between MATLAB and OpenDSS at Buses 6, 7, and 9 were then compared, as summarized in Table VI.

TABLE VI
VALIDATION ERROR BETWEEN MATLAB AND OPENDSS

Case	Bus 6 Error (%)			Bus 7 Error (%)			Bus 9 Error (%)			Total Q
	a	b	c	a	b	c	a	b	c	(MVar)
Base	0.005	0.006	0.005	0.022	0.016	0.009	0.021	0.018	0.009	0
1 (Bus 3)	0.008	0.020	0.010	0.068	0.089	0.089	0.080	0.108	0.108	179
2 (PSO-PS)	0.010	0.020	0.020	0.070	0.070	0.089	0.070	0.090	0.109	57.62
3 (GA)	0.010	0.020	0.030	0.090	0.090	0.119	0.099	0.099	0.128	82.85

As shown in Table VI, the discrepancy between MATLAB and OpenDSS simulations across all cases ranged from 0.005% to 0.128%, with an average error of 0.053%. These results indicate strong consistency, supporting the validity of the proposed modeling and simulation framework.

V. CONCLUSION

This paper presents an integrated framework for optimal STATCOM placement in industrial power systems, combining metaheuristic optimization with MATLAB-based simulation and OpenDSS cross-validation. Through a sequential application of PSO, GA, and PS, the framework identifies appropriate STATCOM sizing and placement under steady-state conditions to minimize reactive power demand while maintaining voltage regulation. The results show that STATCOM installations near load buses enhance voltage support, while optimized multiple placements can reduce reactive power requirements by up to 67.81% compared with single installations, thereby providing practical preliminary guidelines for STATCOM sizing. Moreover, the sequential optimization strategy demonstrates improved performance in higher-dimensional problems.

Future work will extend the proposed framework to incorporate advanced STATCOM control strategies and dynamic operating conditions that consider contingency scenarios. In addition, the applicability of the sequential optimization approach will be further investigated for large-scale and more complex power systems, including those with renewable energy sources.

REFERENCES

[1] Electric Power Research Institute, "The cost of power disturbances to industrial and digital economy companies," Palo Alto, CA, Jun. 2001.

[2] U.S. Environmental Protection Agency, *Inventory of U.S. Greenhouse Gas Emissions and Sinks: 1990–2022*, EPA 430-R-24-004, Apr. 2024.

[3] U. Mumtahina, S. Alahakoon, and P. Wolfs, "A literature review on the optimal placement of Static Synchronous Compensator (STATCOM) in distribution networks," *Energies*, vol. 16, no. 17, Art. no. 6122, 2023.

[4] H. Mun, *Optimal Placement of Dynamic Voltage Restorers and Static Synchronous Compensators for Enhancing Power Quality*, M.S. thesis, The Univ. of Texas at Austin, Austin, TX, USA, 2025.

[5] G. Choudhary, N. Singhal, and K. S. Sajan, "Optimal placement of STATCOM using crow search algorithm," in *Proc. ICCCCM*, 2016.

[6] N. G. Hingorani and L. Gyugyi, *Understanding FACTS: Concepts and Technology of Flexible AC Transmission Systems*. Piscataway, NJ, USA: Wiley–IEEE Press, 2000.

[7] H. Mun, D. Zccheviki, S. Santoso, and L. Jiang, "Improving power quality of industrial plants using dynamic voltage restorers," in *Proc. 2025 IEEE PESGM*, Austin, TX, USA, July 2025.

[8] Electric Power Research Institute, *Transmission Line Reference Book: 345 kV and Above*, EPRI, 1982.

[9] U.S. Dept. of Agriculture, "REA Bulletin 50-4: 34.5/19.9 kV Line Construction," Nov. 1986.

[10] R. C. Dugan and S. Santoso, "An example of 3-phase transformer modeling for distribution system analysis," in *Proc. IEEE PES Transmission and Distribution Conf. and Exposition*, 2003, pp. 1028–1032.

[11] J. J. Grainger and W. D. Stevenson, *Power System Analysis*. New York, NY, USA: McGraw-Hill, 1994.

[12] I. Kocar, J. Mahseredjian, U. Karaagac, G. Soykan, and O. Saad, "Multiphase load-flow solution for large-scale distribution systems using MANA," *IEEE Trans. Power Del.*, vol. 29, no. 2, pp. 908–915, Apr. 2014.

[13] National Fire Protection Association, *NFPA 70: National Electrical Code*. Quincy, MA, USA: NFPA, 2020.

[14] J. Kennedy and R. C. Eberhart, "Particle swarm optimization," in *Proc. IEEE Int. Conf. Neural Netw. (ICNN)*, Perth, Australia, 1995.

[15] D. E. Goldberg, *Genetic Algorithms in Search, Optimization, and Machine Learning*. Reading, MA: Addison-Wesley, 1989.

[16] C. Audet and J. E. D. Jr., "Analysis of generalized pattern searches," *SIAM J. Optim.*, vol. 13, no. 3, pp. 889–903, 2003.

979-8-3315-8138-1